

Supporting Information

The shape anisotropy of magnetic nanoparticles: an approach to cell-type selective and enhanced internalization

*Tanja Potrč¹, Slavko Kralj^{*1,2,3}, Sebastjan Nemeč^{1,2}, Petra Kocbek¹ and Mateja Erdani Kreft^{*4}*

¹ Faculty of Pharmacy, University of Ljubljana, 1000 Ljubljana, Slovenia

² Department for Materials Synthesis, Jožef Stefan Institute, 1000 Ljubljana, Slovenia

³ Nanos SCI, Nanos Scientifacae d.o.o., Teslova 30, 1000 Ljubljana, Slovenia

⁴ Institute of Cell Biology, Faculty of Medicine, University of Ljubljana, 1000 Ljubljana, Slovenia

1. Materials

The chemicals used for the syntheses of superparamagnetic particles were of reagent grade quality and were obtained commercially. The preparation of the nanoparticle clusters and magnetic nanochains was based on iNANOvative™ platform developed by Nanos SCI company (Ljubljana, Slovenia). Iron (III) sulphate hydrate, iron (II) sulphate heptahydrate (ACS, 99%), citric acid (99%), and NH₄OH (25%) were supplied by Alfa Aesar (Lancashire, UK). Polyacrylic acid (PAA,

30 wt% solution, MW 30 kDa) was purchased from PolySciences GmbH (Hirschberg an der Bergstrasse, Germany). Acetone (AppliChem GmbH, Darmstadt Germany) and ethanol absolute (Carlo Erba, reagent, USP, Milan, Italy) were used without further processing. Hydroxy (polyethyleneoxy) propyl triethoxysilane (silane-PEG, 8-12 EO, 50% in ethanol) was supplied by Gelest Inc. (Morrisville, PA, USA). Tetraethoxysilane (TEOS; 98%), (3-aminopropyl) trimethoxysilane (APS; 97%), rhodamine B isothiocyanate (RB) dichloromethane (DCM), dimethylformamide (DMF), and polyvinyl pyrrolidone (PVP, 40 kDa) were obtained from Sigma Aldrich (St. Louis, MO, USA).

2. Methods

2.1. Synthesis of magnetic nanoparticles

Individual nanocrystals of superparamagnetic iron oxide in the form of maghemite ($\gamma\text{-Fe}_2\text{O}_3$), were prepared by co-precipitation of Fe^{2+} and Fe^{3+} ions from an aqueous solution, as reported elsewhere.¹⁻³ Briefly, ferrous sulfate (FeSO_4) and ferric sulfate ($\text{Fe}_2(\text{SO}_4)_3$) were dissolved in distilled water to obtain final concentrations of 0.027 mol L^{-1} of Fe^{2+} and 0.014 mol L^{-1} of Fe^{3+} . Next, the nucleation was triggered with aqueous ammonia (~25%). First, the pH was set to 3 and kept constant at that value for 30 min. After that time period, the pH was set to 11.7. After additional 30 min, the formed nanocrystals were collected by magnetic separation and washed five times with an aqueous ammonia solution at pH 10.2, then finally dispersed in 80 mL of water. The washed nanocrystals were further functionalized with citric acid. A volume of 5 mL of a 0.5 g mL^{-1} citric acid aqueous solution was added to the nanocrystal suspension in 80 mL of water, and the pH was adjusted to 5.2 with aqueous ammonia. The reaction mixture was then stirred at 450 rpm in an oil bath at $80 \text{ }^\circ\text{C}$ for 90 min. After that, the pH was set to 10.2 with aqueous ammonia. Finally, the

obtained suspension was centrifuged at 5000 g for 5 min to remove any aggregated nanocrystals while the supernatant, representing the ferrofluid, was used for further procedures.

2.2. Synthesis of fluorescent superparamagnetic nanoparticle clusters (SNCs)

SNCs were synthesized in an emulsion-based system where a large number of 10 nm maghemite nanocrystals were self-assembled into spherical clusters by using polyacrylic acid and polyvinylpyrrolidone, as reported elsewhere.^{4,5} The precise control of the cluster size was obtained by size sorting using a high-gradient magnetic separator (HGMS). The synthesis procedures were developed by Nanos SCI and know-how is suitably protected. The nanocrystal clusters were coated with a layer of silica⁴. For fluorescent labelling, rhodamine B isothiocyanate (RB) was covalently bonded into the matrix of the silica shell. The reaction between RB and APS was carried out separately in the mixture of DCM/DMF = 4/1 overnight at room temperature. Briefly, RB (0.00933 mmol) was dissolved in the DCM/DMF solvent mixture (0.5 mL) and then APS (0.186 mmol) was added. After the reaction completion, the volatile solvent was removed using argon flow and the product (RB-APS) was mixed with TEOS for the fluorescent silica coating. In brief, 160 mg of the nanocrystal clusters with fluorescent thin silica shell were dispersed in 80 mL of ethanol and 2 mL of ammonia. Then, 0.52 mL of TEOS was added into the reaction mixture while stirred for 3h. Finally, the synthesized SNCs with a 25-nm-thick silica shell were magnetically separated from the suspension and washed with ethanol and then 3-times with distilled water.

2.3. Synthesis of fluorescent superparamagnetic nanochains (CHAINS)

The synthesis procedure of nanochains is fully described elsewhere.⁶⁻⁹ It is based on dynamic magnetic assembly approach where multiple parameters are precisely defined in order to control the nanochains length. Briefly, nanochains composed of approximately 7 nanoparticle clusters

were synthesized as follows. First, the aqueous suspension of nanocrystal clusters (2.3×10^{-8} M) was dispersed into aqueous polyvinylpyrrolidone (PVP, molecular weight 40 kDa, pH 4.3 adjusted by HCl, final concentration 1.25×10^{-4} M) solution and then exposed to a homogeneous magnetic field (70 ± 15 mT). The reaction mixture was stirred with glass propeller at 220 rpm during the synthesis. Dynamic magnetic assembly of nanocrystal clusters is directed by the fine tuning between the magnetic alignment and shear stress disruption which result in the formation of linear chain-like structures in the suspension. A TEOS (final concentration 45 mM) was added to the mixture 10 min after the transfer of nanocrystal clusters into the PVP solution. For fluorescent labelling, RB was covalently bound into the matrix of the silica shell. The reaction between RB and APS was carried out separately in the mixture of DCM/DMF = 4/1 overnight at room temperature. Briefly, RB (0.00933 mmol) was dissolved in the solvent mixture (0.5 mL) and then APS (0.186 mmol) was added. Subsequently, the volatile solvent was removed using argon flow and the product (RB-APS) was mixed with TEOS for the fluorescent silica coating. The magnetically aligned nanocrystal clusters were permanently fixated with a layer of deposited silica. Subsequently, 160 mg of the fluorescent nanochains were dispersed in 80 mL of ethanol and 2 mL of ammonia. Then, 0.50 mL of TEOS was added into the reaction mixture while stirred for 3h. The silica coating (thickness 25 nm) was completed within 3 h, after which the coated nanochains (CHAINS) were magnetically separated from the suspension and washed twice with ethanol and 3-times with distilled water.

2.4. Functionalization of magnetic nanoparticles with polyethylene glycol (PEG)

The surfaces of the fluorescent silica-coated nanoparticle clusters (SNCs) and nanochains (CHAINS) were modified by direct one-step functionalization with silane-PEG molecules. In brief, magnetic particles (150 mg, 15 mL distilled water) were diluted with 15 mL of ethanol to which

75 μL of silane-PEG and 250 μL of aqueous ammonia were added while the reaction mixture was stirred mechanically with glass propeller at 400 rpm for 5 h at 55 $^{\circ}\text{C}$. The synthesized SNC-PEG and CHAIN-PEG were magnetically separated from the suspension and washed first with ethanol, twice with distilled water, and dispersed in distilled water.

2.5. Characterization of magnetic nanoparticles

The particle nanostructures were assessed by transmission electron microscopy (TEM). The 10 μL drop of nanoparticle suspension was deposited on a copper grid (SPI, West Chester, USA) coated with perforated carbon foil. Then, the suspension deposited on the grid was air-dried prior to TEM analyses. The analyses were performed with a transmission electron microscope (Jeol JEM 2100, Jeol, Akishima, Japan) operating at 200 kV. The magnetic properties of the nanoparticles were measured at room temperature by vibrational sample magnetometry (VSM) (Lake Shore 7307 VSM, Lake Shore Cryotronics, Westerville, OH, USA). The zeta potential measurements were carried out at a final particle concentration of 0.1 mg mL^{-1} in an aqueous solution containing KCl (final concentration of 10 mM). Zeta potential measurements were performed on Zeta PALS, Brookhaven Instruments Corporation, Holtsville, NY, USA. The hydrodynamic size distribution of the synthesized spherical nanoparticle clusters (SNCs) was measured by dynamic light scattering (DLS) (Fritsch, Analysette, Germany). For the measurements, the colloidal suspensions were diluted with corresponding buffer to achieve optimum count rate.

2.6. Normal and cancer urothelial biomimetic and co-culture models

The normal and cancer urothelial models were cultured in the following culture media. Human bladder invasive urothelial neoplasm (T24) cells were grown in A-DMEM/F12 (1:1) (Gibco), 5% fetal bovine serum (FBS; Gibco) (FBS), 4 mM glutamax (Gibco), 100 U mL^{-1} penicillin, and 100

$\mu\text{g mL}^{-1}$ streptomycin and were maintained at 37 °C in a humidified 5% CO₂ atmosphere for 1 week before experiments. Normal primary urothelial (NPU) cells were grown in the UroM medium, prepared as described below.^{10,11}

Primary and secondary cultures of NPU cells were established from three porcine urinary bladders (biological replicates), which were obtained from a local abattoir, as described previously¹². Briefly, each porcine urinary bladder was cut into stripes and urothelial cells were gently scraped with a scalpel blade. Cells were seeded in tissue culture flasks and grown in UroM medium. UroM medium consisted of equal parts of MCDB153 medium (Sigma-Aldrich) and A-DMEM (Invitrogen), and was supplemented with 0.1 mM phosphoethanolamine (Sigma-Aldrich), 15 $\mu\text{g mL}^{-1}$ adenine (Sigma-Aldrich), 0.5 $\mu\text{g mL}^{-1}$ hydrocortisone (Sigma-Aldrich), 5 $\mu\text{g mL}^{-1}$ insulin (Sigma-Aldrich), 4 mM glutamax (Invitrogen), 100 $\mu\text{g mL}^{-1}$ streptomycin, and 100 $\mu\text{g mL}^{-1}$ penicillin. Passages IV to VII of urothelial cells were used for experiments at a seeding density of 1×10^5 cells/cm².

Since the endocytosis of highly differentiated normal urothelial cells is very low as we have shown in our previous studies,^{10,12-16} we prepared hyperplastic and normoplastic urothelial models and analyzed the endocytosis of nanoparticles into the cells of both models. For the establishment of the partially differentiated urothelial model, which resembles the hyperplastic urothelium *in vivo*, the cells were grown in UroM medium containing 2.5% FBS and with an extracellular calcium concentration of 0.9 mM, i.e. UroM (-Ca²⁺ + S_{FBS}). For the establishment of the highly differentiated urothelial model, which resembles the normoplastic urothelium *in vivo*, the cells were grown in UroM medium without FBS and with physiological calcium concentration of 2.7 mM, i.e. UroM (+Ca²⁺ - S_{FBS}).^{16,17} The models were maintained at 37 °C in a humidified 5% CO₂ atmosphere for 3 weeks before experiments.

The cells were for 24 h exposed to nanoparticles ($100 \mu\text{g mL}^{-1}$) in the same culture medium as used for establishment/differentiation of urothelial cell models. The control samples were grown in the specific culture media without addition of nanoparticles.

To further analyze the differences in the extent of intracellular accumulation of nanoparticles, we established a co-culture model of urothelial cancer and normal cells, as described in our recent study¹⁸. In co-cultures, NPU cells were seeded at a seeding density of 5×10^4 and T24 cells at 5×10^3 cells/cm². On day 1 of growth, cells were exposed to nanoparticles ($100 \mu\text{g mL}^{-1}$) in UroM medium for 24 h. After 24 h the co-cultures were washed with UroM medium and prepared for phase-contrast and fluorescence microscopy.

The experiments with urothelial cells were approved by the Veterinary Administration of the Slovenian Ministry of Agriculture and Forestry in compliance with the Animal Health Protection Act and the Instructions for Granting Permits for Animal Experimentation for Scientific Purposes.

2.7. Cellular uptake of magnetic nanoparticles and their impact on cell morphology

Transmission electron microscopy

Normal and cancer urothelial models were prepared as described previously.¹⁹ The cells were fixed with 4% (w/v) formaldehyde (Sigma) and 2.5% (v/v) glutaraldehyde (Serva, Heidelberg, Germany) in 0.1 M cacodylate buffer, pH 7.4 for 2 h 45 min. The fixation was followed by overnight rinsing in 0.1 M cacodylate buffer and post-fixation in 2% (w/v) osmium tetroxide for 1 h at room temperature. Afterwards, the samples were incubated in 2% uranyl acetate (Merck, Germany) for 1 h at room temperature. The samples were then dehydrated in a graded series of

ethanol and embedded in Epon (Serva). Epon semi-thin sections were stained with 1% toluidine blue and 2% borate in distilled water and observed with a Nikon Eclipse TE microscope. Ultrathin sections were contrasted with uranyl acetate and lead citrate and observed with a transmission electron microscope (Philips CM100, (Philips, Eindhoven, Netherlands), operation voltage 80 kV, equipped with CCD camera (AMT, Danvers, MA, USA)). The thickness of each ultrathin section is up to 70 nm, which is less than a diameter of single spherical nanoparticle cluster from which the nanochains are prepared. The nanochains are thus inevitably sliced during the sample preparation procedure and cannot retain the intact structure.

For transmission electron analysis, 7-20 high-quality micrographs of 350 μm^2 surface (with 1-5 cells per micrograph, depending on the urothelial model and magnification) were acquired and magnetic nanoparticle uptake and cell morphology were analyzed.

Fluorescence microscopy

Normal and cancer urothelial models as well as the co-culture model of urothelial cancer and normal cells were fixed in 4% formaldehyde (w/v) for 15 min. The cells were then washed in PBS for 30 min and mounted onto slides. The samples were examined with the phase contrast and fluorescence microscope (Nikon Eclipse) and the AxioImager.ZI microscope (Carl Zeiss MicroImaging GmbH, Heidelberg, Germany; 63X oil immersion objective, numerical aperture 1.4). However, the correlative phase contrast and fluorescence images were taken with the same microscope (Nikon Eclipse). Red channel values corresponded to the intensity of the fluorescence of endocytosed nanoparticles. We obtained fluorescence images (2560 \times 1920 pixels, 600 dpi). To estimate the apparent size of compartments (particles) containing SNC-PEGs or CHAIN-PEGs, the fluorescence images of the samples were analyzed with the ImageJ software. The image was

thresholded at 50% of the maximum intensity value. The minimum size of a fluorescent spot taken to identify an individual nanoparticle-positive compartment was two adjacent pixels ($0.98 \times 0.49 \mu\text{m}$), and the minimum surface area covered by a punctum was $0.48 \mu\text{m}^2$. This way, a broad span of particles containing SNC-PEGs or CHAIN-PEGs with different apparent sizes was covered by the analysis.

2.8. The effects of magnetic nanoparticles on cell viability

Due to multilayer nature of urothelial models, Trypan blue viability assay was used to determine the viability of urothelial cells after nanoparticle exposure. The cells were grown in 6-well plates until urothelial models were established and then incubated with $100 \mu\text{g mL}^{-1}$ nanoparticles for 24 h. After incubation, cells were washed to remove non-internalized nanoparticles, trypsinized until all cells were detached and following manufacturer's instructions immediately stained with Trypan blue dye, which labels only dead cells. Live and dead cells were then counted manually under inverted light microscope (Leica). The percentage of viable cells (% Viability) in a given sample was determined as the ratio between the number of viable cells in the sample (NS) and the number of all cells in the non-treated control (N0) for each cell model: % Viability = $100 \times \text{NS} / \text{N0}$. Three independent experiments were conducted, each in three or six technical replicates for each urothelial model.

2.9 Thermogravimetric analysis

Thermogravimetric analysis (TGA) was performed for SNC, SNC-PEG, CHAIN, CHAIN-PEG and PEG-silane. The sample (10 mg) was weighted in an alumina crucible and analyzed in the temperature range from $30 \text{ }^\circ\text{C}$ to $650 \text{ }^\circ\text{C}$ in an inert atmosphere (nitrogen flow 50 mL/min) at a heating rate of $10 \text{ }^\circ\text{C/min}$, using a thermogravimeter TGA/DSC 1 STARe System (Mettler-Toledo;

Greifensee, Switzerland). The PEG content was determined based on weight loss in the temperature range from 150 °C to 500 °C.

2. 10 Inductively coupled plasma mass spectrometry (ICP-OES)

Since we have demonstrated the difference between nanoparticle uptake between cancerous urothelial cells and highly differentiated normal urothelial cells, we also wanted to investigate whether there was a difference between cancerous and not fully differentiated normal urothelial cells. Therefore, we made partially differentiated normal urothelial models and compared their Fe uptake with the cancerous urothelial model. The normal and cancerous urothelial models were cultured for 7 days in the culture media described in section 2. 6. After 7 days, normal NPU and cancerous T24 cells were incubated with 100 µg/mL SNC-PEGs or CHAIN -PEGs for 24 h and then cell viability was determined with trypan blue staining. The iron content in the cells was determined using ICP-OES analysis. Nine technical replicates (in nine 6-well plates) were performed for each urothelial model.

Total concentrations of Fe in the analyzed samples were determined using Agilent 5800 VDV ICP-OES instrument (Agilent Technologies, Tokyo, Japan). Standard solution of Fe was diluted with water for the preparation of fresh calibration standard solutions. To determine the concentration of Fe in cell cultures, the nanoparticle-treated cell cultures were collected (we combined three samples together) by centrifugation at a speed 200 g for 5 min. The supernatant was discarded and the cell sediment was redispersed using ultrasonication in 100 µl of concentrated HCl (~37 %; ~12 M). The formed dispersion was kept in a hot water bath (1003, GFL, Burgwedel, Germany) at 80 °C for 48 h and sonicated every few hours using an ultrasonication bath (Sonis 4, IskraPIO, Ljubljana, Slovenia). The dispersion was then diluted to a final volume of 12 mL with MilliQ

water. Prior the ICP-OES determination of Fe content the samples were further diluted as necessary. For the calculation of cellular uptake, the endogenous Fe (control groups without nanoparticles) was subtracted (marked as Corrected C_{Fe}). In addition, we calculated total mass of Fe (μg) based on corrected C_{Fe} and mean mass of Fe per cell.

3. Results

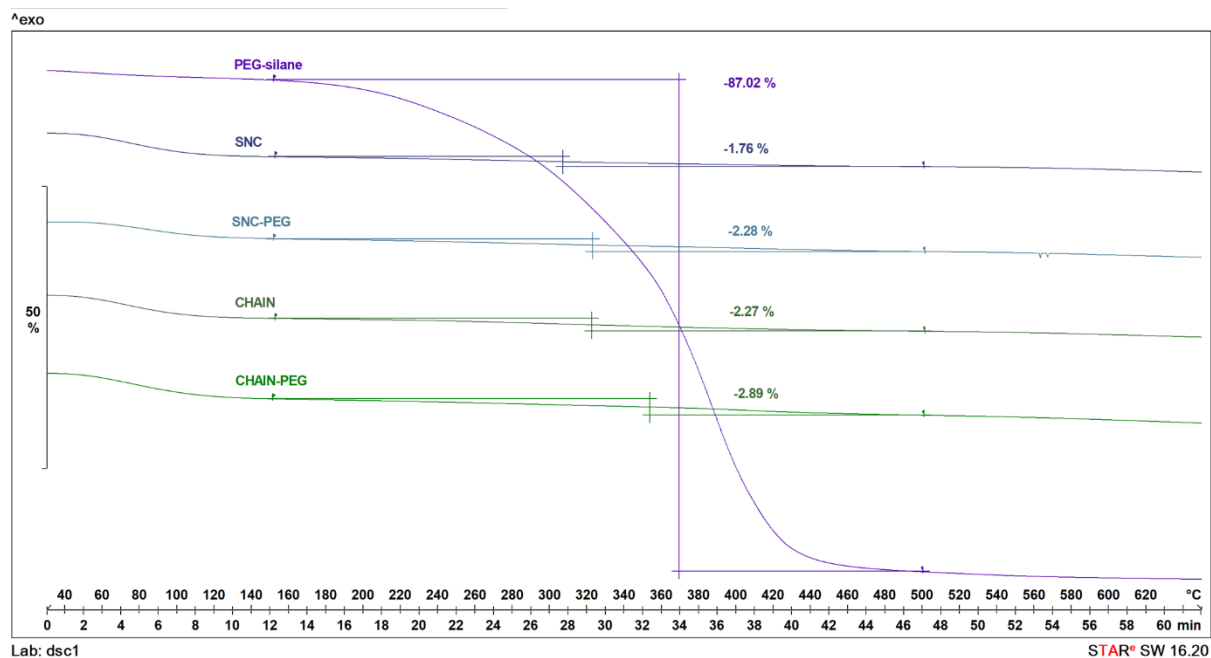


Figure S1: Representative graphs of the weight loss during the TGA of PEG-silane, SNC, SNC-PEG, CHAIN and CHAIN-PEG.

REFERENCES

- 1 S. Kralj, D. Makovec, S. Čampelj and M. Drofenik, *J. Magn. Magn. Mater.*, 2010, **322**, 1847–1853.
- 2 S. Kralj, M. Rojnik, J. Kos and D. Makovec, *J. Nanoparticle Res.*, 2013, **15**, 1666.
- 3 S. Kralj, M. Drofenik and D. Makovec, *J. Nanoparticle Res.*, 2011, **13**, 2829–2841.
- 4 M. Tadic, S. Kralj, M. Jagodic, D. Hanzel and D. Makovec, *Appl. Surf. Sci.*, 2014, **322**, 255–264.

- 5 S. Kralj, F. Longobardo, D. Iglesias, M. Bevilacqua, C. Tavagnacco, A. Criado, J. J. Delgado Jaen, D. Makovec, S. Marchesan, M. Melchionna, M. Prato and P. Fornasiero, *ACS Appl. Nano Mater.*, 2019, **2**, 6092–6097.
- 6 S. Kralj and D. Makovec, *ACS Nano*, 2015, **9**, 9700–9707.
- 7 M. Tadic, S. Kralj, Y. Lalatonne and L. Motte, *Appl. Surf. Sci.*, 2019, **476**, 641–646.
- 8 M. Tadic, S. Kralj and L. Kopanja, *Mater. Charact.*, 2019, **148**, 123–133.
- 9 L. Kopanja, M. Tadić, S. Kralj and J. Žunić, *Ceram. Int.*, 2018, **44**, 12340–12351.
- 10 J. Lojk, V. B. Bregar, K. Strojjan, S. Hudoklin, P. Veranič, M. Pavlin and M. E. Kreft, *Histochem. Cell Biol.*, 2018, **149**, 45–59.
- 11 T. Višnjar, P. Kocbek and M. E. Kreft, *Histochem. Cell Biol.*, 2012, **137**, 177–186.
- 12 U. D. Jerman, T. Višnjar, I. H. Bratkovič, N. Resnik, M. Pavlin, P. Veranič and M. E. Kreft, *Int. J. Mol. Sci.*, 2021, **22**, 5565.
- 13 M. E. Kreft, R. Romih, M. Kreft and K. Jezernik, *Differentiation*, 2009, **77**, 48–59.
- 14 M. Pavlin, J. Lojk, V. B. Bregar, M. Rajh, K. Mis, M. E. Kreft, S. Pirkmajer and P. Veranic, *Int. J. Nanomedicine*, 2015, 1449.
- 15 L. Tratnjek, R. Romih and M. E. Kreft, *Histochem. Cell Biol.*, 2017, **148**, 143–156.
- 16 D. Zupančič, M. E. Kreft, M. Grdadolnik, D. Mitev, A. Iglič and P. Veranič, *Protoplasma*, 2018, **255**, 419–423.
- 17 T. Višnjar and M. E. Kreft, *Vitr. Cell. Dev. Biol. - Anim.*, 2013, **49**, 196–204.
- 18 N. Resnik, D. Baraga, P. Glažar, Š. Jokhadar Zemljič, J. Derganc, K. Sepčić, P. Veranič and M. E. Kreft, *Front. Cell Dev. Biol.*, , DOI:10.3389/fcell.2022.934684.
- 19 A. Janev, T. Ž. Ramuta, L. Tratnjek, Ž. Sardoč, H. Obradović, S. Mojsilović, M. Taskovska, T. Smrkolj and M. E. Kreft, *Front. Bioeng. Biotechnol.*, , DOI:10.3389/fbioe.2021.690358.